Solid Freeform Fabrication 2019: Proceedings of the 30th Annual International
Solid Freeform Fabrication Symposium – An Additive Manufacturing Conference
Reviewed Paper

INFLUENCE OF POWDER PARTICLE SIZE DISTRIBUTION ON THE PRINTABILITY OF PURE COPPER FOR SELECTIVE LASER MELTING

M. Sinico[1,2], G. Cogo[2], M. Benettoni[2], I. Calliari[3], and A. Pepato[2]

[1] Department of Mechanical Engineering, KU Leuven, 3001 Leuven, BE
[2] National Institute for Nuclear Physics - Padova Division, 35131 Padova, IT
[3] Department of Industrial Engineering, University of Padova, 35131 Padova, IT

Abstract

This work investigates the use of fine Cu powder, with ~ 20 vol% smaller than 15 μm size, for the selective laser melting process. Cubes reaching > 98 % density are produced at relative low laser output (175 W) and characterized. After the selection of a proper combination of laser scan parameters, the properties of fabricated parts are briefly studied through profilometry and tensile tests. Finally, a voluminous demo component for high-energy physics is manufactured to stress-test the employed SLM machine. Even though unmolten particles and lack of fusion defects are still present in the produced specimens, the investigated approach confirms that powder selection can have a huge influence on the processability of materials with high reflectivity towards near-infrared irradiation.

Introduction

Selective Laser Melting, also called Laser Powder Bed Fusion, is an Additive Manufacturing technique designed to use a high power laser to melt and fuse metallic powders together in a layer-by-layer fashion. The process has seen a considerable industrial adoption during recent years, thanks to the possibility to produce freeform near-net shape components with low material waste and reduced design-to-production time [1].
Despite the advantages of this fabrication technique, limitations are still present with one main restriction being the available material palette. Only few materials are currently used at an industrial scale, with many more studied at academic level, due to the fact that SLM is a complex multiphysics process, and that the successful SLM fabrication is dependent on a considerable amount of variables. Those variables, with a sub-section of them being the SLM process parameters, need to be fine-tuned to obtain dense and accurate parts with suitable mechanical properties, but the identification of this optimal process windows is often time and resource intensive. Moreover, the material needs to be available in powder form with a specific granulometry and high sphericity.
One of the materials of interest that still poses some obstacles for its effective SLM fabrication is pure copper. Copper not only suffers from its most known properties, with a higher tendency of melt pool instability during SLM due to the rapid dissipation of the deposited heat input. It is also one of the materials with the highest reflectivity towards the near-infrared radiation, which corresponds to the emitted wavelength region of commonly adopted lasers in SLM systems (continuous wave fiber lasers). This poses serious troubles on its effective SLM fabrication, since only a fraction of the irradiated power is absorbed and contributes to the melting process, leading to a porous component with many unmolten particles. Various researchers during the years have suggested diversified approaches to successfully fabricate this difficult material, and the most common ones to date are to use copper alloys or a mixture of powders with copper particles and other elements to increase the absorbance in the infrared at the cost of electrical and thermal conductivity [2]. Other solutions have been the implementation of green or blue lasers in SLM machines [3], since the reflectivity of copper decreases with wavelength from the infrared through ultraviolet regions, or the use of powerful fiber lasers up to 2000 W [4,5,6]. None of the latter proposed solutions have been industrially accepted, on account of the fact that the common available SLM machines do not support these kind of options and should be modified individually at a cost. All the attempts at a lower laser power [7,8] using CO_2 or standard fiber lasers have failed, never reaching a density of the produced pure copper parts higher than 90 %.

The SLM of pure copper material could unlock the possibility to produce innovative heat exchangers with enhanced thermal conductivity [1], complex induction coils with increased electrical conductivity [9], and many other components like heat sinks in injection molding, copper anodes for fuel cells, and miscellaneous parts [10] where thermal and electrical properties are more of a concern. This demand arises not only from the industry, but also from different fields of academic research like experimental physics or aerospace, where the adoption of SLM could lower the design-to-production time of unique components that are nowadays produced with several steps of standard manufacturing processes, will all the connected limitations. The AM of copper in these research fields has already being spotted as a solution e.g. for components in the DEMO (DEMOnstration power plant) and ITER (International Thermonuclear Experimental Reactor) fusion power plants [11], or 3D printed rocket thrust chambers [10].

In this work, the influence of powder particle size distribution is studied and correlated to the SLM processability of pure copper. It is well known [12,13] that powder granulometry influences the SLM printability: fine spherical particles with a wide enough size distribution are reported to be easier to be molten in respect to coarser ones, generally increasing powder bed packing density and favoring part densification. In addition, the particle size should be tuned on the employed SLM layer thickness to promote an homogeneous spread of the powder layer. On the other hand, fine powders also present lower flowability, caused by their higher tendency towards cohesion and agglomeration due to stronger inter-particle attractive forces, and an increased chemical reactivity, e.g. higher propensity to oxidation. Consequently, there should always be a balance between the positive (e.g. easier melting process) and negative (e.g. decreased flowability) effects of introducing finer particles in the SLM process, to maximize the quality of the printed part.
As depicted before, machine modifications (green-blue lasers, high power fiber lasers) and raw material modifications (alloying elements) have been already explored as possible solutions for copper SLM production, while the combination of fine powder with a thin layer thickness has never been reported in literature. Our hypothesis is that, despite the high reflectivity, this combination of favorable conditions could ease the melting process of pure copper, allowing to decrease the total amount of porosities in the final printed part. To test our hypothesis, one standard pure copper powder for SLM and one engineered distribution of fine copper powder have been acquired and processed, with the results hereby reported in the following essay.

Powder characterization

Two gas atomized pure copper powders (99.8 wt% Cu) with different powder particle distributions have been purchased from LPW Technology Ltd. The first distribution, hereby called Cu 15-45, is the standard size distribution being sold by the supplier. The second distribution, hereby called Cu 10-35, has been engineered in collaboration with the supplier to meet defined constraints. Specifically, the engineered powder should be suitable to be deposited in building layers of 20 µm. Therefore, the D50 of the powder distribution is requested to be around the employed layer thickness, while the D90 should be below the effective layer thickness. D50 and D90 are the values of the particle diameter at 50 % and 90 % in the cumulative distribution, respectively. The effective layer thickness t_{eff} is calculated assuming a powder layer density of 60 % [13], and corresponds to 33.3 µm.
Laser diffraction analyses have been provided by the supplier after the atomization of the two powders (Figure 1), confirming that the Cu 10-35 engineered distribution meets the requirements. Moreover, the presence of a tail of smaller particles, with a volume below 15 µm of 21.31 %, is considered positive and will generally help to fill the voids between coarser particles and consequently increase the powder bed packing density and ease the melting process [12].
Scanning Electron Microscopy (SEM) inspection has also been performed, and is reported in Figure 1. From the captured SEM images it can be noticed that the majority of particles exhibits a spherical shape, along with a limited amount of irregularly shaped particles. The standard distribution Cu 15-45 seems to present a lower mean sphericity and a slightly discernible higher amount of satellites compared to the engineered distribution Cu 10-35.

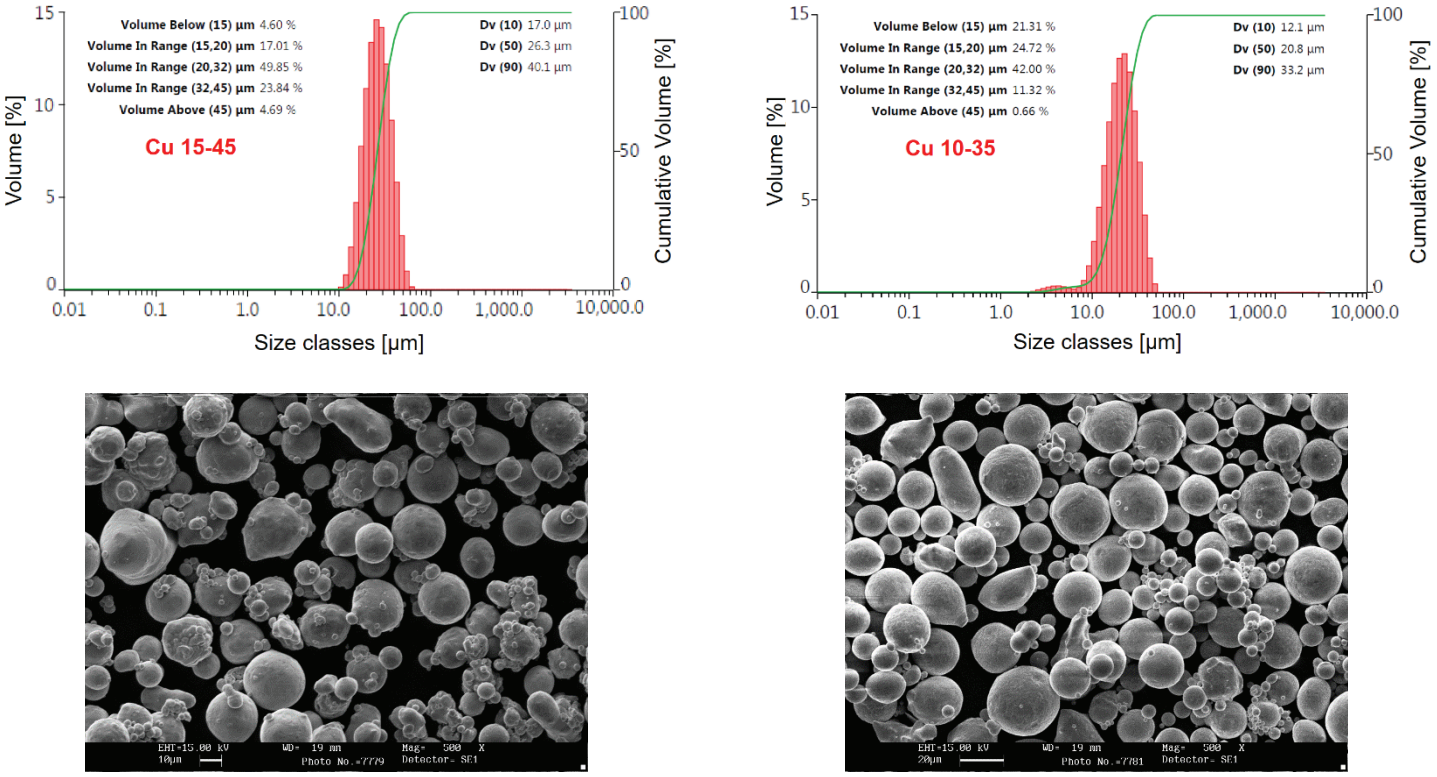

Figure 1. Particle size distribution (PSD) of the selected pure copper powders, from laser diffraction analyses (provided by LPW Technology Ltd); corresponding SEM images below each PSD.

Finally, laser absorption measurements were carried out on a Jasco V-570 spectrophotometer with integrating sphere ISN-470 (λ max range 200-2000 nm). The baseline correction for the measurements has been performed on the provided barium sulfate white board. Results for the two copper distributions (Figure 2) are compared with results acquired on stainless steel 316L and bronze CuSn10 powders gently provided by the company SISMA S.p.A.

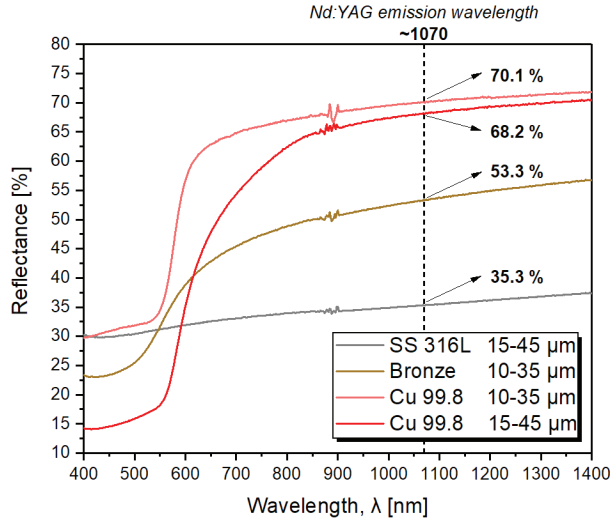

Figure 2. Laser absorption measurements via spectrophotometer of the selected pure copper powders, and of stainless steel 316L and bronze CuSn10 powders for comparison.

The optical reflectance of the used copper powder bed is ~70 % at a wavelength of 1070 nm (near-infrared) for both Cu distributions. This result is comparable to previous reported laser absorption measurements [4,14] and confirms one of the main challenges of SLM copper production. It is worth noticing how the engineered Cu 10-35 powder actually presents a slighter higher reflectance, probably due to a higher powder bed packing

density which could lower the multiple internal reflections and subsequent absorption of the optical light between separate particles. The difference in reflectance is better compared with the bronze CuSn10 powder, where the presence of Sn in 10 wt % in the alloy is able to decrease the reflectance from ~70 % to ~53 %, further evincing why copper alloys have been more successfully processed with the current market of SLM machines [2,15,16].

SLM setup and experimental methodology

The performance of the two copper powders have been evaluated with the production of specimens through a SISMA mysint100 PM SLM machine. The main advantage of the selected system relies on the small laser spot size of ~30 µm, which helps to increase the total energy density on the surface of the powder bed ($E_s = P/(v \times d)$ with P laser power, v laser scanning speed and d laser spot size). The 200 W fiber laser of the machine emits infrared radiation at ~1070 nm, and it is therefore expected a total reflection from the copper powder as depicted in Figure 2. The system main characteristics are summarized on Table 1.

Table 1. Technical specifications of the employed SISMA mysint100 PM SLM machine.

Technical Data	mysint100
Building volume	Ø 100 mm x 100 mm
Laser source	Fiber Laser 200 W
Precision optics	Quartz F-Theta Lens
Laser spot diameter	30 µm laser
Typical layer thickness	20 µm - 40 µm (adjustable)
Power supply	220-240 V 1ph - 50/60 Hz
Max power absorbed	1,53 kW
Inert gas	Nitrogen, Argon
Inert gas supply	6 mm / 2.5 ÷ 5bar @ 35 L/min
Inert gas consumption	<0,3 L/min @ 0,5% O_2
O_2 concentration	O_2: <100ppm
Machine dimensions	1390 mm x 777 mm x 1600 mm (LxWxH)
Net weight	650 kg

Cubic specimens 10x10x10 mm (example in Figure 3a) have been produced with both Cu 15-45 and Cu 10-35 powders, at a fixed laser power of 175 W. The laser power has been fixed to that value to maximize the surface energy density E_s; the maximum power of 200 W has not been used to prevent precocious wear of the laser source, given the high scheduled amount of experiments.

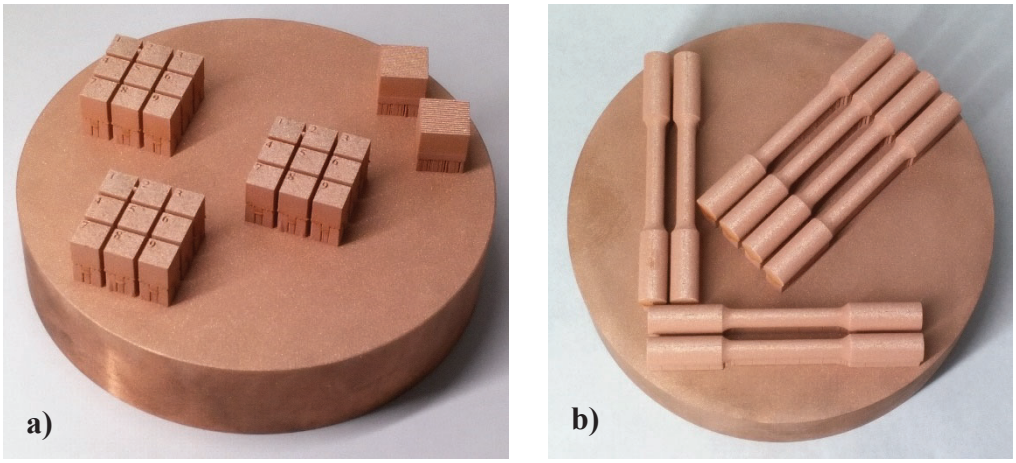

Figure 3. a) Example of 27 10x10x10 mm specimens arrangement on the build platform ($\varnothing_{platform}$ = 99 mm) for SLM parameters optimization study; b) example of horizontal tensile test specimens arrangement.

Layer thickness has been as well fixed to a value of 20 µm, whereas laser scanning speed, hatch spacing and scanning pattern have been varied. No powder flowability issues have been encountered while using the Cu 10-35 fine powder distribution, and a standard rubber recoating system has been enough to provide homogeneous powder layers during SLM processing in nitrogen atmosphere.
Relative density measurements have been performed, after careful cutting and polishing of the cubes, with optical microscopy and, for selected specimens, SEM inspection. Moreover, chemical etching through a mixture of 2.5 g $FeCl_3$ – 1 ml HCl – 100 ml EtOH have been employed to highlight observed lack of fusion porosities. All the samples have been built on top of a specifically designed copper OFHC platform.
After SLM parameters optimization, specimens for tensile tests (example in Figure 3b) and surface roughness measurements have been fabricated with the Cu 10-35 powder batch. The tensile samples have been designed following the ASTM E8M - 16a standard (test piece diameter d_o = 4 mm) and tested in as-build condition on a MTS 858 Mini Bionix II with a displacement rate of 2 mm/min. A MTS extensometer 632.29F-30 with a gage length of 5 mm was used to measure the strain during the tensile tests. Finally, an optical profiler Sensofar PLu neon has been employed for the roughness analyses, following the ISO 4287-1997 standard.

Results and discussion

SLM processing

The SLM parameters optimization is summarized in Figure 4, where obtained relative densities of the cubic specimens after optical measurement are compared between the two Cu powders and plotted as a function of volumetric energy density ($E_v = P/(v \times h \times t)$ with P laser power, v laser scanning speed, h hatch spacing and t layer thickness). A full analysis of the dependence of relative density on the different set of parameters, e.g. v, h, scanning pattern, is scheduled to be published in a full journal paper.

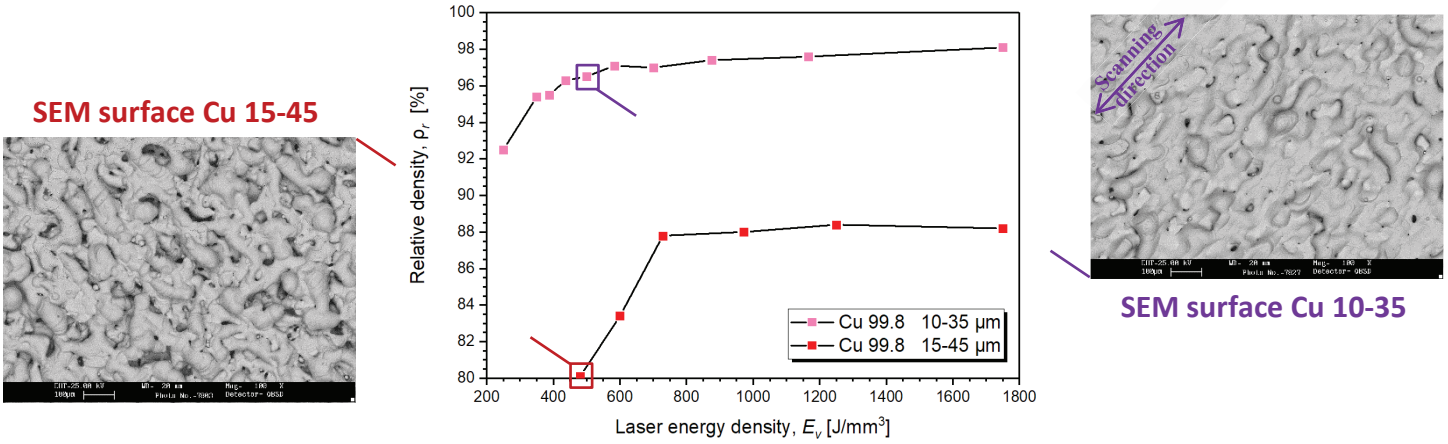

Figure 4. SLM parameters optimization for the two Cu powders, relative densities are plotted as a function of E_v; two SEM images (100x magnification) of top surfaces are appended for selected specimens.

The maximum obtained relative density for Cu 15-45 is 88.4 %, in line with previous published literature on the SLM processing of pure copper [7,8]. On the other hand, the selected Cu powder presents an impressive improvement in densification, with a maximum value of 98.1 %. From SEM inspection of top surfaces, the Cu 15-45 specimens can be described as a porous structure with melting beads and almost non-distinguishable laser line tracks. Cu 10-35 specimens, instead, have a stable fusion and more continuous line tracks, even if some balling, recesses and weld interruptions remain. To identify the causes of the remaining porosity content in the Cu 10-35 samples, etching has been performed and an example can be seen in Figure 5.

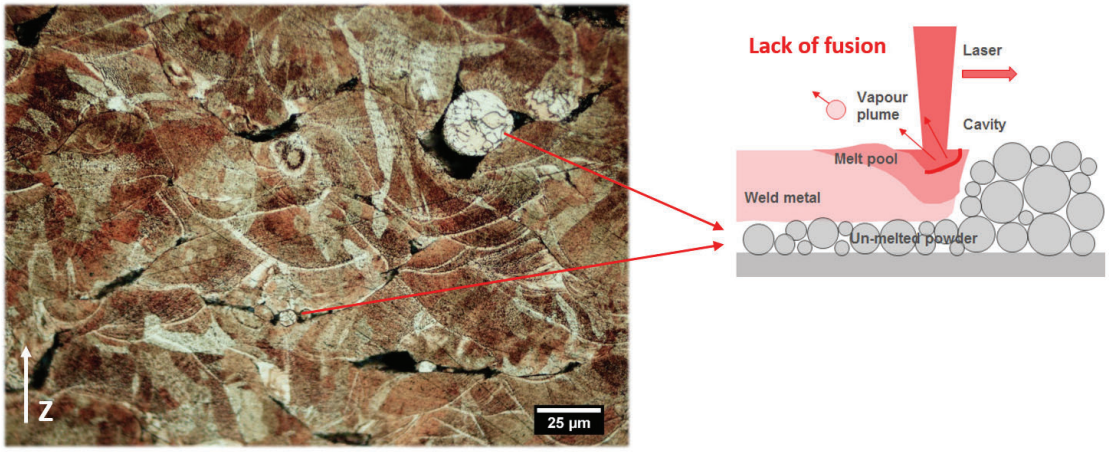

Figure 5. Optical inspection of a selected Cu 10-35 specimen (from Figure 3) after etching of a Z cross section, i.e. building direction; lack of fusion drawing courtesy of [17].

It's clear from the etched sample that lack of fusion still compromises the successful SLM production of pure copper. Even if a higher relative porosity is achieved with the selected powder, semi-molten particles and "knit" weld lines between subsequent layers are not completely avoided. Lower mechanical properties, e.g. strength and ductility, in the Z direction (anisotropy) and an overall low fatigue life of components are to be expected. Tests are ongoing to evaluate the electrical and thermal conductivity of the samples with the highest relative density in respect to the IACS standard. We believe that parts produced with the optimized set of parameters can't be certified for applications that might require intensive mechanical load, but could nevertheless possibly be adopted for specific applications where electrical and thermal conductivity are more of a concern. It remains anyhow impossible at this stage to draw conclusions before the complete characterization of the samples.
As a final remark, it is imperative that a more in-depth analysis of the total porosity content should be done, with the comparison of the obtain values from optical inspection against Archimedes method and possibly micro Computed Tomography. Although the Struers guidelines [18] have been followed during the metallographic preparation of the specimens, the possibility of deformation caused by the grinding and polishing steps could partially hide the smaller pores and thus falsely lower the porosity content. That said, the investigated approach confirms nonetheless that powder selection can have a huge influence on the SLM processability of pure copper, and powder morphological properties like particle size distribution should preferably always be tuned beforehand on the SLM system and process parameters window, e.g. layer thickness, that are going to be employed.

Mechanical tests and surface roughness measurements

The mechanical tests, performed on series of 8 samples built both on the XY plane (Figure 3b) and on the Z direction (building direction), are summarized in Table 2.

Table 2. Results of the mechanical tests on the SLM fabricate Cu samples, reference values of Cu C11000 properties from [19] for comparison.

	Tensile strength [MPa]	0.2% yield strength [MPa]	Modulus of elasticity [GPa]	Elongation at break [%]
SLM Copper, XY direction	207 ± 26	157 ± 23	133 ± 21	9.83 ± 0.83
SLM Copper, Z direction	130 ± 23	125 ± 19	83 ± 16	2.48 ± 0.43
Reference, C11000 electrolytic tough-pitch Cu, cold-worked (H04 temper)	*345*	*310*	***112*** *- 130*	*12*
Reference, C11000 electrolytic tough-pitch Cu, hot-rolled	*220*	*69*	*112 -* ***130***	*45*

Note: all data points with their corresponding standard deviation.

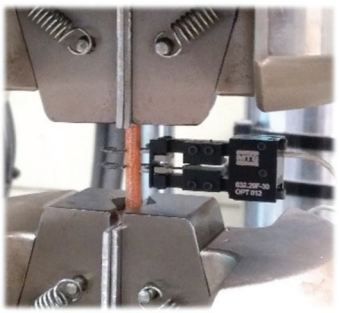

The surface of the specimens was not treated after SLM fabrication (as-built), and only the supports were detached from the parts. The parameter set used for these samples provides a corresponding E_v of ~583 J/mm^3, with an expected relative density of 97.1 % (Figure 4). It was decided to avoid the parameter combinations at higher E_v since their volumetric material fabrication rate was too low to be applicable at an industrial scale.
As per our knowledge, the only reported mechanical test on pure copper fabricated by SLM was 149 MPa of ultimate tensile strength for a relative density of the sample of 88.1 % (XY direction) [7]. In this work, a tensile strength of 207 MPa is achieved for the horizontal XY direction, further corroborating the improvement of our proposed approach. Overall, the obtained XY properties are analogous or superior than C11000 electrolytic tough-pitch Cu in hot-rolled condition. The major drawback is solely the percentage of elongation, which -mostly due to the remaining porosities and lack of fusion defects- halts at a value of ~10 %.
This behavior is more accentuated for the samples built in the Z direction, where all measured mechanical attributes deteriorate considerably. More specifically, the tensile strength drops to a value of 130 MPa while the percentage of elongation decreases to ~2.5 %. As predicted, lack of fusion is a typical defect that diminishes the bonding between SLM layers, and therefore lowers the mechanical properties of printed parts in the Z direction. Fabricated objects will experience extensive anisotropy and an expected low fatigue life. It must be specified that the influence of minor alloying elements (0.2 wt%), crystal structure, crystal orientation, phases or strain in the material are not accounted for and they could as well have a considerable impact on the reported measurements. It is well known [4,8] that SLM copper commonly presents a fine grained microstructure and might display a crystallographic texture due to the generated temperature gradients within the melt pools. Both of these microstructural contributions should be further investigated to better understand and predict the mechanical behavior of SLM copper material.

Finally, the surface roughness analyses performed on a rhombohedral specimen are shared on Figure 6. The specimen is produced with the same parameters used for the mechanical test samples. Each reported roughness measurement has been repeated at different locations on each surface, taking care that the profiles are measured perpendicular to the typical lay lines featured on SLM surfaces, i.e. the laser line tracks.

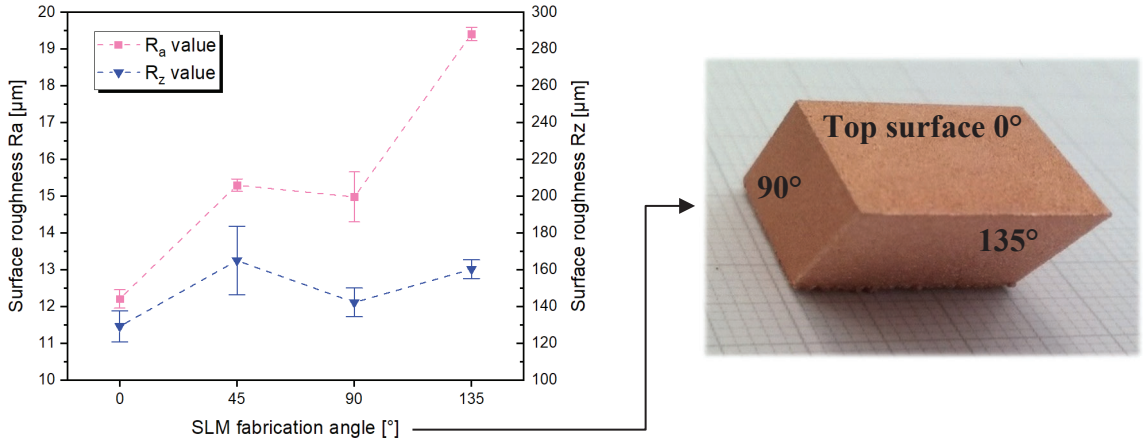

Figure 6. Surface roughness measurements of the Cu 10-35 rhomboid at different SLM fabrication angle, all data points reported with their standard deviation.

The R_a results, with 12.21 ± 0.25 µm for the top surface, are comparable with the standard surface quality achieved by common SLM machines [20] and therefore reflect the improved melting and higher relative density of the Cu 10-35 samples. The trend of the surface roughness at different angles is also reasonable, with a decrease in surface quality for sloped surfaces where the staircase effect comes into play. In addition, for the 135° surface, the combination of the staircase effect with being a downfacing region considerably worsens the surface condition.
However, more information can be retrieved if attention is put on the R_z parameter and not on the arithmetical mean deviation parameter R_a, that is by definition an average. It is then noticed how actually R_z, or the maximum height of the roughness profile, is mildly higher than regular [20] probably due to the fact that -even with an

improved melting- some balling, surface porosities and laser tracks irregularities remain in the samples. Those features, as shown before in the SEM image (Figure 4), will determine few larger peaks and valleys in the roughness profile which consequently reflects better on the maximum height parameter.

SLM stress-test: building a demo component for high-energy physics application

Given the high reflectivity of pure copper (Figure 2) the risk of laser back-reflection is considerably high and has been recently reported in literature [4]. Back reflections can create new focal points inside the optical system during processing and thus damage the optical mirrors, compromising the SLM system. Although this issue is more prone to occur at higher laser powers than the one used in this work (175 W), it is withal deemed paramount to check if the SLM machine can withstand production of massive copper parts. A demo component for high-energy physics is consequently selected for production as the final test-sample of our research; the detailed description and function of the part are not the main subject of this paper and, hence, they will be just briefly described.
The part is a beam dump designed to stop the proton beam of a cyclotron at the end of a beamline [21]. The beam dump has to guarantee the full power heat removal in a safe way fulfilling all the design specifications as well as radio protection limits (examples of beam dump designs in [22,23]). The object can be conceived as a heat exchanger, where the protons are initially decelerated by bulk copper material, and this material must be cooled down to avoid the part to reach its melting temperature and/or have material vaporization inside the beamline. In details, for the proposed application, the component must be able to dissipate ~30 kW of a Gaussian 70 MeV beam power deposited in a beam spot size of 21.4 cm^2 surface area (RMS, ±3 σ). That is equivalent to 1.4 kW/cm^2 of energy that should be removed by a suitable cooling system. The following sketch helps to recap the main concepts.

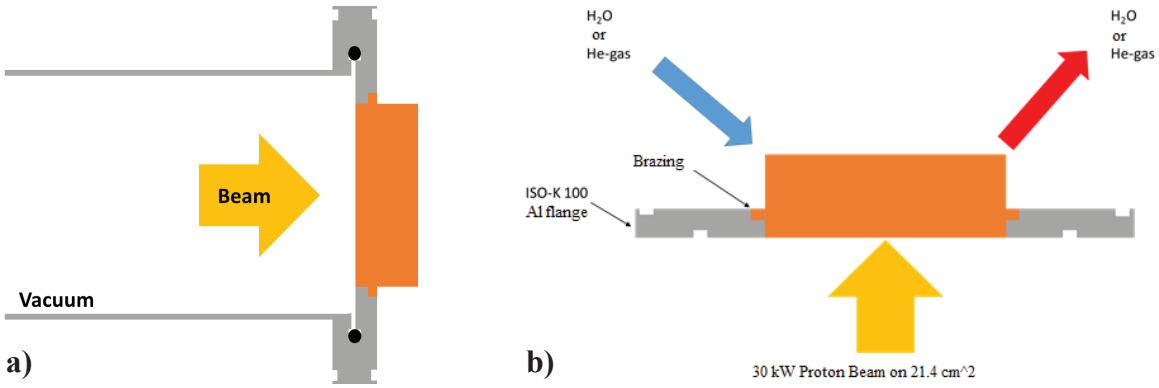

Figure 7. Explanatory sketch of the beam dump purpose,
a) beamline end with the component in orange plus b) details of the design constraints.

To perform the task, the beam dump should have a front portion, facing the beam, composed of bulk dense copper to effectively stop the incoming protons, and a second back portion where the cooling system acts to cool down the front. The thickness of the front portion, dependent on the stopping power of the material [24] and on the incident beam properties, is estimated to be ~8 mm for Cu OFHC (Monte Carlo SRIM-2013 simulation [25]).
Since, as previously reported, the SLM of pure copper still cannot output fully dense parts, the beam dump front side is directly obtained from the Cu OFHC platform, where the higher purity and density of the material enhance its thermal conductivity and stopping power. Only the cooling system, designed in a spiral way to remove the generated heat from the center of the component all the way to the outer sides, has been 3D printed on top of the Cu OFHC platform. Figure 8a portraits the main idea, with 10 mm (8*1.25 safety factor) of bulk high purity copper in the front portion. The AM design freedom is adopted for the conformal cooling spiral channel, as well as -potentially- the implementation of a metallic foam e.g. metallic struts inside the channel itself to increase the turbulence of the cooling liquid. This design and manufacturing approach saves production steps and, if the

enhanced thermal efficiency is proved, could be a viable way to create a smaller and lighter beam dump compared to the conventionally manufactured ones presented in scientific literature [22,23].
The part has been fabricated with a production set of SLM parameters, to keep the overall production time at a reasonable level. The corresponding E_v of ~365 J/mm^3 is consequently lower than the obtained one for the tensile test specimens. The 3D printed cooling system has a total volume of 88392 mm^3, with a printing height Z of 32 mm. The top surface of the OFHC platform has been sandblasted prior to production to avoid laser back reflections from the polished surface of the platform itself, given the 90.1 % reflectance for polished or electroplated pure copper surfaces [19].

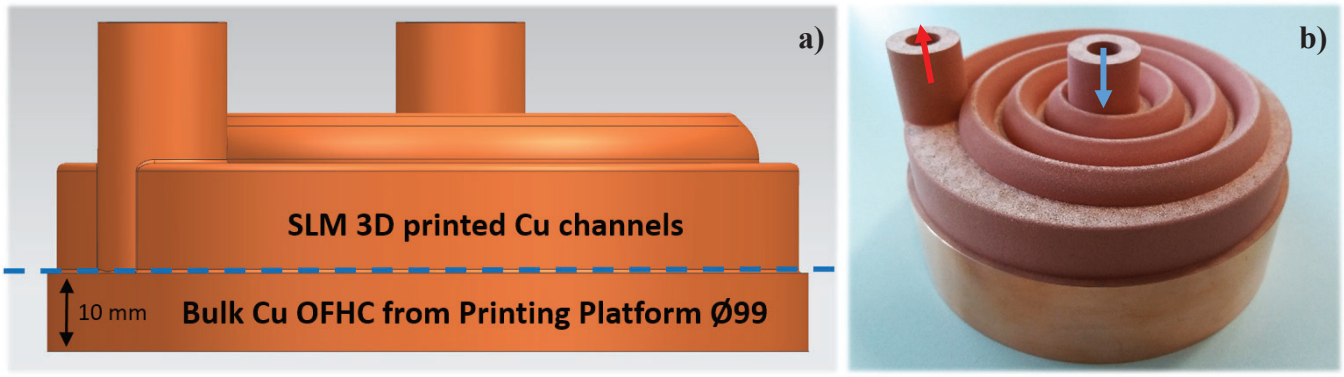

Figure 8. a) Side view of the CAD design, highlighting the 10 mm bulk Cu OFHC from the building platform; b) beam dump after successful SLM production, with its spiral cooling system.

In Figure 8b, a photo of the beam dump after SLM manufacturing is shown. The part was successfully produced in one single job of ~75 hours. No major drawbacks were noticed during the SLM phase, and after the positive result of this stress-test the same SISMA mysint100 PM machine was later employed to produce other Cu showcases and demo components.
We want to disclose that the beam dump case study hereby described has been designed as a demo part as well, based on real data from the SPES cyclotron project [21]. The goal was to highlight AM and specifically SLM copper production potential for high-energy physics applications, and further design iterations, simulations and tests will be necessary to develop the final product.

Conclusions

Pure copper specimens and demo-components have been fabricated by Selective Laser Melting reaching a relative density of 98.1 %. A novel approach has been suggested to overcome the difficulties encountered in the AM laser production of copper, combining the use of a fine Cu powder (in the range of 10-35 µm) and a small layer thickness to ease the melting process with standard fiber lasers and reduce the lack of fusion defects. Comparing the obtained results against standard size powder (15-45 µm) processed at the same combinations of SLM parameters, it has been demonstrated how powder selection is the critical factor and should always be tuned beforehand based on the SLM machine, processing conditions, and material. The proposed approach yet cannot achieve full density parts, with lack of fusion defects still present in the processed samples. Anyhow, the diminished total porosity content confirms that the use of powders with a PSD skewed towards finer particles is effective to manufacture relatively high density pure copper parts at a laser power lower than 200 W.
Moreover, complete mechanical properties have been reported for SLM fabricated pure copper for the first time in both horizontal and building direction. The measured properties, combined with the good obtained as-build surface quality, confirm once more the initial hypothesis of this work. Analogous or superior mechanical strength than C11000 electrolytic tough-pitch Cu in hot-rolled condition can be achieved for the horizontal fabricated specimens, while in the building direction the tensile strength and elongation at break drop due to the lack of fusion between building layers. In view of the anisotropic behavior, the produced parts probably cannot be certified for applications that might require intensive mechanical load, but could nevertheless possibly be adopted for specific functions where electrical and thermal conductivity are more of a concern.

Hence, a voluminous demo component for high-energy physics has been fabricated as a proof-of-concept of a possible thermal application and to stress-test the SLM machine in use. The part was successfully built in ~75 hours, and no critical laser back-reflection or any complication occurred during the build job.
Further studies are ongoing to obtain a more in-depth analysis of the total porosity content in correlation to the applied scanning parameters and strategies; furthermore, the influence of minor alloying elements, crystal structure, crystal orientation, phases or strain in the material should be investigated to better understand their contribution to the measured mechanical properties. Finally, the electrical and thermal conductivity of the fabricated copper samples with the highest relative density are being measured, and will be reported and discussed in a forthcoming journal paper.

Acknowledgements

This research was supported by the project 5687-1-2121-2015 POR FSE 2014-2020 Veneto "Implementation and characterization of advanced additive manufacturing techniques, applied to the production cycle of the mechanical industry in the Veneto Region". The industrial partners SISMA S.p.A. and Officina Dei Materiali SaS are kindly acknowledged for the continuous guidance and training throughout the project and for giving access to their laboratories and equipment. We would also like to express our gratitude to Eng. Daniele Rigon and Prof. Giovanni Meneghetti, who performed the tensile tests at the Department of Industrial Engineering, University of Padova. Moreover, assistance provided by Eng. Matteo Bellin for the roughness measurement was greatly appreciated. Finally, special thanks to Dr. Juan Esposito for the fruitful discussions on the beam dump design constraints and the magic of cyclotrons.

References

[1] T. T. Wohlers, I. Campbell, O. Diegel, R. Huff, J. Kowen, *Wohlers Report 2019*, Wohlers Associates Inc., March 2019.

[2] C. Y. Yap *et al.*, 'Review of selective laser melting: Materials and applications', *Applied Physics Reviews*, vol. 2, no. 4, Dec. 2015.

[3] M. Tsukamoto, S. Masuno, Y. Sato, R. Higashino, K. Tojo, and K. Asuka, 'Development of high intensity blue diode laser system for materials processing', in *High-Power Diode Laser Technology XVI*, San Francisco (US), 2018.

[4] S. D. Jadhav, S. Dadbakhsh, L. Goossens, J.-P. Kruth, J. Van Humbeeck, and K. Vanmeensel, 'Influence of selective laser melting process parameters on texture evolution in pure copper', *Journal of Materials Processing Technology*, vol. 270, pp. 47–58, Aug. 2019.

[5] M. Colopi, L. Caprio, A. G. Demir, and B. Previtali, 'Selective laser melting of pure Cu with a 1 kW single mode fiber laser', *Procedia CIRP*, vol. 74, pp. 59–63, 2018.

[6] T.-T. Ikeshoji, K. Nakamura, M. Yonehara, K. Imai, and H. Kyogoku, 'Selective Laser Melting of Pure Copper', *JOM*, Dec. 2017.

[7] P. A. Lykov, E. V. Safonov, and A. M. Akhmedianov, 'Selective Laser Melting of Copper', *Materials Science Forum*, vol. 843, pp. 284–288, Feb. 2016.

[8] F. Trevisan, F. Calignano, M. Lorusso, M. Lombardi, D. Manfredi, and P. Fino, 'Selective laser melting of chemical pure copper', *Proceedings of Euro PM 2017*, Milano (MI), IT, Oct. 2017.

[9] GKN Additive, 'Reduce your induction hardening coil costs through 3D printing', *GKN Powder Metallurgy White Paper*, 2019.

[10] F. Singer, D. C. Deisenroth, D. M. Hymas, and M. M. Ohadi, 'Additively manufactured copper components and composite structures for thermal management applications', in *2017 16th IEEE Intersociety Conference on Thermal and Thermomechanical Phenomena in Electronic Systems (ITherm)*, Orlando, FL, 2017, pp. 174–183.

[11] S. J. Zinkle, 'Applicability of copper alloys for DEMO high heat flux components', *Physica Scripta*, vol. T167, Feb. 2016.

[12] J. H. Tan, W. L. E. Wong, and K. W. Dalgarno, 'An overview of powder granulometry on feedstock and part performance in the selective laser melting process', *Additive Manufacturing*, vol. 18, pp. 228–255, Dec. 2017.

[13] A. B. Spierings and G. Levy, 'Comparison of density of stainless steel 316L parts produced with selective laser melting using different powder grades', *Proceedings of the Annual International Solid Freeform Fabrication Symposium,* The University of Texas, Austin (TX), US*,* p. 20, Aug. 2019.

[14] D. Q. Zhang, Z. H. Liu, S. Li, M. Muzzammil, C. H. Wong, and C. K. Chua, 'Selective Laser Melting: On the Study of Microstructure of K220', *Proceedings of the 1st International Conference on Progress in Additive Manufacturing (Pro-AM 2014)*, pp. 176-184, 2014.

[15] A. Popovich, V. Sufiiarov, I. Polozov, E. Borisov, D. Masaylo, and A. Orlov, 'Microstructure and mechanical properties of additive manufactured copper alloy', *Materials Letters*, vol. 179, pp. 38–41, Sep. 2016.

[16] D. Palousek *et al.*, 'SLM process parameters development of Cu-alloy Cu7.2Ni1.8Si1Cr', *Rapid Prototyping Journal*, vol. 25, no. 2, pp. 266–276, Mar. 2019.

[17] M. Saunders, 'X marks the spot - find ideal process parameters for your metal AM parts', *White papers collection – Renishaw plc*, Sept. 2017.

[18] E. Weidmann, A. Guesnier and Struers ApS, 'Metallographic preparation of copper and copper alloys', *Struers ApS Application Notes*, Mar. 2019.

[19] J. R. Davis and ASM International, Eds., *Copper and copper alloys*. Materials Park, OH: ASM International, 2001.

[20] M. Brandt (Ed.), 'Laser Additive Manufacturing: Materials, Design, Technologies, and Applications', *Woodhead Publishing*, 2017.

[21] M. Maggiore et al., 'SPES: A new cyclotron-based facility for research and applications with high-intensity beams', *Mod. Phys. Lett. A*, vol. 32, no. 17, p. 1740010, Jun. 2017.

[22] D. Iglesias *et al.*, 'The IFMIF-EVEDA accelerator beam dump design', *Journal of Nuclear Materials*, vol. 417, no. 1–3, pp. 1275–1279, Oct. 2011.

[23] C-S. Gil, J. H. Kim, D. H. Kim, and J-H. Jang, 'Beam dump development for a Korean proton accelerator', *Proceedings of HB2010 conference*, Morschach, Switzerland, pp. 563-566, 2010.

[24] C-S. Gil, D. H. Kim, and J. Kim, 'Activation Analyses of Beam Dump Materials Irradiated by 100-MeV Protons', *Journal of the Korean Physical Society*, vol. 50, no. 5, pp. 1396-1398, May 2007.

[25] J. F. Ziegler, M. D. Ziegler, and J. P. Biersack, 'SRIM – The stopping and range of ions in matter (2010)', *Nuclear Instruments and Methods in Physics Research Section B: Beam Interactions with Materials and Atoms*, vol. 268, no. 11–12, pp. 1818–1823, Jun. 2010.